Experimental probing of the anisotropy of the empty *p* states near the Fermi level in MgB_2

R. F. Klie[a] and Y. Zhu
Brookhaven National Laboratory, Upton, New York 11973

G. Schneider
Institut fuer Allgemeine Physik und Center for Computational Materials Science (CMS), Technische Universität Wien, A-1060 Wien, Austria

J. Tafto
Department of Physics, University of Oslo, P.O. Box 1048 Blindern, 0316 Oslo, Norway

(Received 31 January 2003; accepted 15 April 2003)

We have studied the boron *K* edge in the superconductor MgB_2 by electron energy loss spectroscopy (EELS) and experimentally resolved the empty *p* states at the Fermi level that have previously been observed within an energy window of 0.8 eV by soft x-ray absorption spectroscopy. Using angular-resolved EELS, we find that these states at the immediate edge onset have p_{xy} character in agreement with predictions from first-principle electronic structure calculations. © *2003 American Institute of Physics.* [DOI: 10.1063/1.1583132]

MgB_2 has received much attention since the discovery of its unexpectedly high superconducting transition temperature of 39 K.[1] Ground-state electronic structure calculations[2–4] have determined that the boron states near the Fermi level predominantly have a *p* character. Additionally, density functional theory (DFT) calculations (Fig. 1)[4] suggest that the p_{xy} states exhibit a high density up to 0.8 eV above the Fermi level before dropping to near zero and then begin to rise again after about 4 eV. The incompletely filled p_{xy} states at the Fermi level onset are believed to play an important role in the superconductivity of this two-dimensional electron-hole Bardeen–Cooper–Schrieffer superconductor. Figure 1 further shows that including the core-hole effect will primarily lead to a decrease of the high density of p_{xy} states at the Fermi level onset. The states with p_z character exhibit a flat density of states over the range of 10 eV from the Fermi level onset. X-ray absorption spectroscopy (XAS) and electron energy loss spectroscopy (EELS) will probe these *p* states in the B *K* edge. Angle averaged soft XAS of the B *K* edge exhibits a peak at the edge onset that is consistent with a high density of *p* states.[3,4] By using polarized x-rays, the symmetry of these states (i.e., whether they are p_{xy} or p_z states) can be determined. However, these experiments require large single crystals, and, to date, x-ray absorption experiments have yet to be performed on such crystals.

Angle-resolved EELS, an alternative to XAS, relies upon analysis of high-energy electrons that have undergone momentum transfer by propagating through a thin specimen. Although conventional transmission electron microscopes (TEM) lack energy resolution in comparison to XAS, the increased spatial resolution of EELS provides an invaluable tool for probing the local electronic structure of polycrystalline materials. Leapman *et al.*[5] have further achieved high angular resolution in a TEM by simultaneously observing the EELS spectrum as a function of scattering angle and energy loss. However, this type of experiment requires large sample areas of constant thickness and crystal orientation. As MgB_2 does not have a prominent cleavage plane, it is difficult to find sample areas that are thin enough for EELS studies and larger than 100 nm in diameter even if the bulk specimens have been thinned by ion milling or similar means. Thus, in order to obtain a good signal-to-noise ratio, we must usually sacrifice the very high angular resolution.

Several recent EELS studies[4,6–8] have attempted to separate the p_{xy} and p_z states in the *B K* edge of MgB_2, by measuring the anisotropy in the fine structure for two incident beam directions, namely parallel and perpendicular to the crystal *c* axis. Under these conditions, a small angular spread of the incident beam as well as the collected electrons (i.e., collection angle <1 mrad for 100 keV) is crucial. These angles must be even smaller at higher acceleration voltages. Due to these demands, there is thus far, no unambiguous

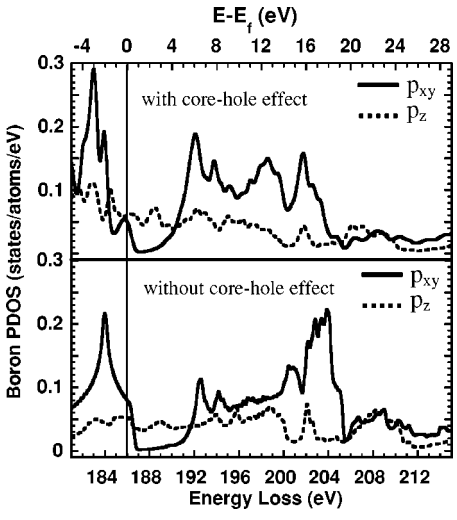

FIG. 1. DFT ground-state calculations of the density of boron p_{xy} and p_z above the Fermi level (bottom). The core-hole effect is included in the top calculations.

[a]Electronic mail: klie@bnl.gov

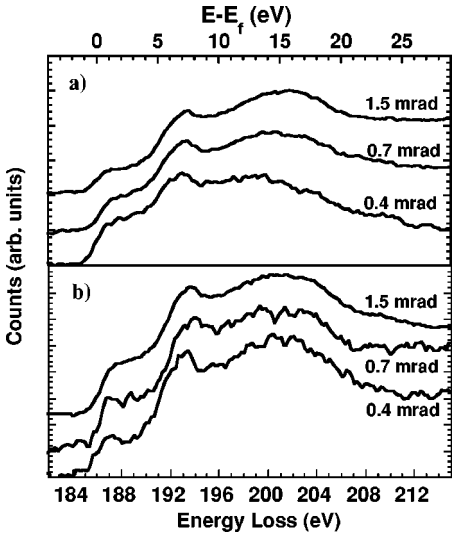

FIG. 2. (a) EELS spectra recorded with the incident beam along the *c* axis with effective collection angles of 0.4, 0.7, and 1.5 mrad. (b) EELS spectra recorded with the incident beam perpendicular to the *c* axis with effective collection angles of 0.4, 0.7, and 1.5 mrad. Each spectrum represents the sum of 15 individual spectra, obtained with 2–5 s acquisition time, a dispersion of 0.2 eV/channel, and subsequently background subtracted.

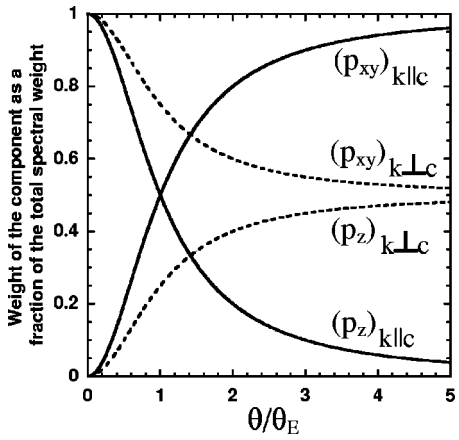

FIG. 3. Fractional contribution from p_z and p_{xy} as a function of scattering angle with the incident beam *k* parallel to the *c* axis ($k \| c$) and incident beam perpendicular to the *c* axis ($k \perp c$). With the incident beam perpendicular to the *c* axis these curves depend on azimutal angle. In this figure, we have averaged over the azimutal angle.

experimental determination of the symmetry of the *p* states just above the Fermi level in MgB_2.

The EELS results were obtained using the JEOL-3000F scanning TEM/TEM, equipped with a Schottky field-emission source operated at 300 keV, an ultrahigh-resolution objective lens pole piece, and a postcolumn Gatan imaging filter. The microscope and spectrometer were setup for TEM with a ''parallel illumination,'' where the convergence angle (α) is chosen to be less than 0.4 mrad and the spectrometer collection angle θ_c variable between 0.4 and 1.5 mrad. 15 individual EEL spectra of the *B K* edge (acquisition time: 2–5 s) are added to increase the signal-to-noise ratio of the near-edge fine structure.

Figure 2(a) shows the B *K* edge with the incident beam parallel to the *c* axis for three different effective collection angles (0.4, 0.7, and 1.5 mrad); Fig. 2(b) shows similar spectra with the incident beam perpendicular to the *c* axis. The shoulder at the edge onset decreases with increasing collection angle in Fig. 2(a), whereas the trend is opposite in Fig. 2(b). Furthermore, in Fig. 2(a), the peak located at 203 eV in the 1.5 mrad spectrum shifts toward the lower end of the spectrum with decreasing collection angle. The opposite can be observed in Fig. 2(b), where the peak shifts from 201 eV in the 1.5 mrad spectrum to 202.5 eV in the 0.4 mrad spectrum. All of these features can be understood by considering the momentum transfer selection of the spectrometer entrance aperture,[8] and the DFT calculations of the B *K* edge.[4] Figure 1 shows that the p_z states have a uniform density of states at the Fermi level, extending more than 5 eV, while the p_{xy} states within this energy window have a high peak at 186 eV with a energy width of 0.8 eV. The highest density of the p_z states can be found at 201 eV, whereas the highest density of p_{xy} states is located at 203 eV.

Figure 3 shows the contribution of p_z and p_{xy} by the momentum transfer parallel and perpendicular to the incident beam direction as a function of scattering angle. Note that these calculations are for discrete scattering directions; to calculate the spectrum for a finite collection angle, we have to consider the cross section variation with scattering angle and integrate over the range of scattering angles.[8] With the incident beam along the *c* axis, as is the case in Fig. 2(a), we thus predominantly probe the p_z states for collection angles smaller than 0.5 mrad, while the contribution from p_{xy} increases with collection angle. For an incident beam parallel to the *c* axis, the p_{xy} contribution approach 100% at large scattering angle. Even at 1 mrad ($\sim 3\ \theta/\theta_E$), an angle well below the regime where the dipole approximation starts to break down, the p_{xy} contribution is already 90%. The trend is different with the incident beam normal to the *c* axis [Fig. 2(b)]. We have to emphasize however, that the anisotropy in the plane with the incident beam normal to the *c* axis necessitates one to average over the azimuthal angle. This will result in a 50% mixture of both the p_{xy} and the p_z contributions.

Significantly larger orientation selectivity can therefore be achieved by displacing the incident beam so that we collect electrons that are scattered at least 0.5 mrad. The entrance aperture of the spectrometer is chosen to correspond to a collection angle in excess of 0.4 mrad. Figure 4 shows two spectra that fulfill these experimental conditions. Spectrum [Fig. 4(a)] is taken with the incident beam perpendicular to the *c* axis, and the center of the entrance aperture is displaced by $\theta_D = 1.2$ mrad toward the (001) diffraction spot; the collection angle ranges from $\theta_c = 0.7$ mrad to $\theta_c = 1.7$ mrad. By displacing the aperture by 1.2 mrad toward the (001) diffraction spot, the majority of the spectral weight is chosen from the p_z contributions. The shape of the B *K* edge exhibits a high intensity prepeak that remains constant over the range of 5 eV, which is in agreement with the first-principle calculations. Although the DFT calculation (Fig. 1) suggest a featureless spectrum for energies up to 15 eV above the Fermi level, a distinct peak at 194 eV, attributable to the remaining p_{xy} contribution, can be seen in the experimental spectrum. Spectrum [Fig. 4(b)] shows the results of the displaced entrance aperture with the *c* axis parallel to the incoming electron beam. The displacement of the aperture is chosen to be $\theta_D = 1.2$ mrad. With the displaced aperture more than 90% of the total spectral contribution originates from

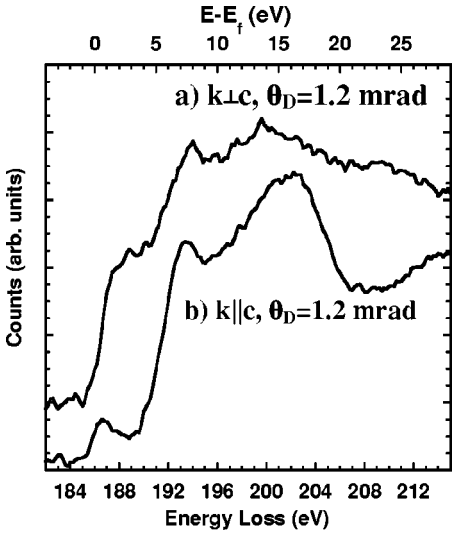

FIG. 4. Spectrum with the incident beam along and perpendicular to the *c* axis. The diameter of the entrance aperture corresponds to an angle of 1.0 mrad and is displaced from the forward direction by 1.2 mrad.

the transitions into the p_{xy} states. We clearly see the pre-edge peak with a high intensity at the edge onset and a subsequent drop in intensity, as predicted from the first-principle calculations. The width of the prepeak of 1.4 eV, can be easily explained as the convolution of the intrinsic peak width of 0.8 eV and the energy spread of the incoming electron beam. Upon further comparison with the DFT calculations (Fig. 1), it is obvious that the high intensity at the edge onset and the relative near-edge fine structure of the B *K* edge can only be explained by disregarding the core-hole effect.

In summary, we demonstrated that the prepeak of the B *K* edge in MgB_2, which was previously mainly attributed to the p_z states, contains contributions from both the p_{xy} and the p_z components for most crystal orientation and acquisition conditions. By choosing the appropriate acquisition conditions, i.e., small collection angle and off-axis spectroscopy, the individual components of the B *K* edge prepeak can be directly separated. The shoulder at the B *K* edge threshold, which originates from transitions into the p_z states decreases with the momentum transfer perpendicular to the *c* axis, whereas a sharp peak just at the Fermi level rises with increasing fraction of the momentum transfer normal to the *c* axis. This leaves little doubt that the peak, previously observed by XAS at the Fermi level,[4] has p_{xy} character in agreement with first-principle calculations without a core-hole effect.

Concluding, we have shown that the p_{xy} peak at the Fermi level can be resolved in the experimental spectra, even with an energy resolution of more than 1.0 eV. This better understanding of the near-edge fine structure of the B *K* edge will allow us to directly evaluate the effects of dopants, point defects, and grain boundaries on the local superconducting charge carrier concentration. Further, the comparison with different kinds of density of states calculations will clarify the importance of the transition matrix elements on the calculated B *K*-edge fine structure.

This work is supported by the U.S. Department of Energy, Division of Materials Sciences, Office of Basic Energy Science, under Contract No. DE-AC02-98CH10886.

[1] J. Nagamatsu, N. Nakagawa, T. Muranaka, Y. Zenitani, and J. Akimitsu, Nature (London) **410**, 63 (2001).
[2] P. Ravindran, P. Vajeeston, R. Vidya, A. Kjekshus, and H. Fjellvåg, Phys. Rev. B **64**, 224509 (2001).
[3] C. McGuinness, K. E. Smith, S. M. Butorin, J. H. Guo, J. Nordgren, T. Vogt, G. Schneider, J. Reilly, J. J. Tu, P. D. Johnson, and D. K. Shuh, Europhys. Lett. **56**, 112 (2001).
[4] Y. Zhu, A. R. Moodenbaugh, G. Schneider, J. W. Davenport, T. Vogt, Q. Li, G. Gu, D. A. Fischer, and J. Tafto, Phys. Rev. Lett. **88**, 247002 (2002).
[5] R. D. Leapman, P. L. Fejes, and J. Silcox, Phys. Rev. B **28**, 2361 (1983).
[6] N. Jiang, B. Jiang, J. C. H. Spence, R. C. Yu, S. C. Li, and C. Q. Jin, Phys. Rev. B **66**, 172502 (2002).
[7] B. Jiang, N. Jiang, and J. C. H. Spence (unpublished).
[8] R. F. Klie, H. Su, Y. Zhu, J. W. Davenport, J. C. Idrobo, N. D. Browning, and P. D. Nellist Phys. Rev. B **67**, 144508 (2003).